Journal of Water Resources and Ocean Science
2025, Vol. 14, No. 1, pp. 1-17
https://doi.org/10.11648/j.wros.20251401.11

Research Article

Appraising the Spatial Relationship Between the Groundwater Physicochemical Quality and the Physiographic Features in the Plateaux Region of Togo

Kossitse Venyo Akpataku[1, 2, 3, *], Akp én èAmenuvevega Dougna[1, 2], Lall ébila Tampo[1, 2], Jean-Marie Dipama[4], Limam Moctar Bawa[2], Masama éya Dadja-Toyou Gnazou[2], Gbandi Djaneye-Boundjou[2], Serigne Faye[3]

[1]Laboratory of Organic Chemistry and Environmental Sciences, Department of Chemistry, University of Kara, Kara, Togo

[2]Laboratory of Applied Hydrology and Environment, University of Lom é, Lome, Togo

[3]Department of Geology, Faculty of Science and Technology, Cheikh Anta Diop University, Dakar Fann, Senegal

[4]Laboratory of Studies and Research on Environments and Territories, University of Ouaga I Pr Joseph Ki-Zerbo, Ouagadougou, Burkina Faso

Abstract

Groundwater is a common drinking water resource worldwide. Understanding the distribution patterns of its chemical constituents is crucial for prioritizing sustainable management strategies. This study aims to present a holistic understanding of the spatial distribution of the physicochemical quality of groundwater in the Plateaux Region of Togo. A hydrochemical database of over 900 borehole water samples was compiled and integrated into GIS tools along with geological, hydrological, soils, land use and land cover, and other ancillary data. Comparison tests, global and local spatial autocorrelation, and hot spot analysis were performed at a confidence level of 95%. The results showed that groundwater is generally fresh and slightly acidic. Our results stress the importance of controlling physiographic features on groundwater quality. The Kruskal-Wallis test revealed statistical differences ($p < 0.05$) among physiographic groups for each groundwater quality parameter. The spatial statistics highlight the spatial dependence in the data and substantial variability in the chemical composition of groundwater due to association with physiographic features. In general, mountainous forest zones with higher rainfall recorded the predominance of lower conductivity values and less contamination in groundwater, probably due to the high rate of groundwater recharge and fast fluxes or circulation driven by topographic gradients. In contrast, those in the south, the center, and sometimes in the east and north present a substantially more advanced mineralization. The High-High clusters are similar and developed southwestward. Fluoride hot spots are associated with groundwater alkalinization in the North and granitoids displaying high-K calc-alkaline magnesian series in the southwest. The hotspots for nitrate concentrations are located at the southeast and northeast ends of the Region due to the affluence of contamination sources and the aquifer vulnerability. This study appears significant as a relevant contributing tool for the sustainable management of groundwater resources in the region.

[*]Corresponding author: akossiv@gmail.com (Kossitse Venyo Akpataku)

Received: 9 December 2024; **Accepted:** 3 January 2025; **Published:** 7 January 2025

Keywords

Fluoride, Groundwater, Nitrate, Plateaux Region, Spatial Statistics, Togo

1. Introduction

As an easily accessible and relatively stable water resource, groundwater is the world's population's primary drinking water source. Also, it provides water for industries, irrigation, and ecosystem equilibrium. However, groundwater quality and use may vary at local or regional scales due to the variation of natural and anthropogenic drivers [1]. Its chemical composition is related to the global water cycle and the characteristics of aquifers and landscapes. A better understanding of groundwater response to environmental factors is required to improve the decisions and management options regarding groundwater quantity and quality-related issues [2-4].

Physiographic variables like topography, drainage, and slope can affect groundwater occurrence and quality [5]. During the last decades, GIS technology has been applied in groundwater studies to present the spatial distribution of the presence or absence of trends in groundwater quality variables [6]. Gao et al. [7] have used geospatial analysis to evaluate the patterns of iodine distribution in drinking water and their association with geological factors in Shandong Province, China. Tu and Xia [8] used spatial statistics to examine the relationships between land use and water quality in eastern Massachusetts, USA. Koh et al. [9] determined the relationships between groundwater quality and various parameters such as topography, hydrology, and land use across Jeju Island, South Korea. One of the geospatial analysis tools for spatial pattern identification is the spatial clustering method using the Getis-Ord Gi* statistics to examine hot spots and cold spots representing the statistically significant clusters of high and low data values, respectively [10-15]. This approach can be helpful, especially for regions with considerable spatial complexity in natural and anthropogenic conditions. Global and local autocorrelations were also used to identify the degree of correlation of a variable with itself over space [15, 16]. Spatial autocorrelation analysis is used to assess a variable's correlation with the spatial location of the variable, which is a match between location similarity and attribute similarity [16]. Local autocorrelation examines how similar or dissimilar values are within a specific neighborhood or local area, while global autocorrelation assesses the overall pattern and structure of spatial relationships across the entire dataset [17]. Understanding these concepts is crucial in spatial analysis as they help identify patterns hidden in aggregated data [11].

The Plateaux Region is one of the five administrative regions of Togo. It has remarkable socio-economic potential, and the development of water resources for drinking, domestic uses, agriculture, and industries plays an important role. However, one of the significant issues in developing water resources is the quality of the water supplied. The spatially varying distribution of chemical concentrations associated with complex environmental and anthropogenic factors challenges groundwater management in the Plateaux Region [18, 19]. Good water quality ensures better health for the population. At the same time, the sustainability of groundwater resource exploitation depends heavily on management focused on the integrity of resources and the ecological balance or ecosystem stability. Therefore, it is necessary to understand the factors controlling water quality and its relationship with aquifers and local physiographic conditions. In this context, we applied Moran's I indices and the Getis-Ord Gi* statistics to examine the spatial variation of groundwater quality and to explore the spatial relationship with physiographic factors in the Plateaux Region of Togo. This study appears helpful in presenting a holistic understanding of the spatial distribution of groundwater quality and its correlation with physiographic features in the study area.

2. Study Area

The Plateaux Region has an area of 16,800 km^2 and is located between longitudes 0°31 and 1°40 E and latitudes 6°29 and 8°20 N (Figure 1). Its population is approximately 1,640,000 inhabitants [20]. The population is essentially rural and lives in rain-fed agriculture. The main food crops are maize, yam, cassava, rice, beans, peanuts, and soya. The annual rainfall varies from 1800 to 1000 mm eastward (Figure 2b). Regarding temperatures, the eastern part is the warmest, with average annual temperatures around 27 °C compared to 25 °C in the west [21]. The Plateaux Region is characterized by a topographic contrast between the east, a lowland area, and the west, a highland area with scattered hills and mountain ranges of varied lengths and heights (Figure 1).

The Plateaux region of Togo is entirely covered by the rocks from the zones of the Pan-African Dahomeyid belt (Figure 2). The external zone is represented by the schists, quartzites, and mica schists of the Atacora structural unit (USA) and the granitoids of the Amlamé-Palimé Pluton (PAP). The suture zone is represented by the ultrabasic and basic massifs of the Atakpamé-Agou axis to the south and the metadiorites of the Mono-Anié-Akaba complex to the north. The internal zone of the Pan-African Dahomeyid belt is essentially composed of a variety of migmatite sandwiched in

micaceous gneisses at the edge of the suture zone and dioritic gneiss to the east of the study area. These gneisses contain granitic intrusions, often appearing along the shear axes where mylonites are developed [22, 23].

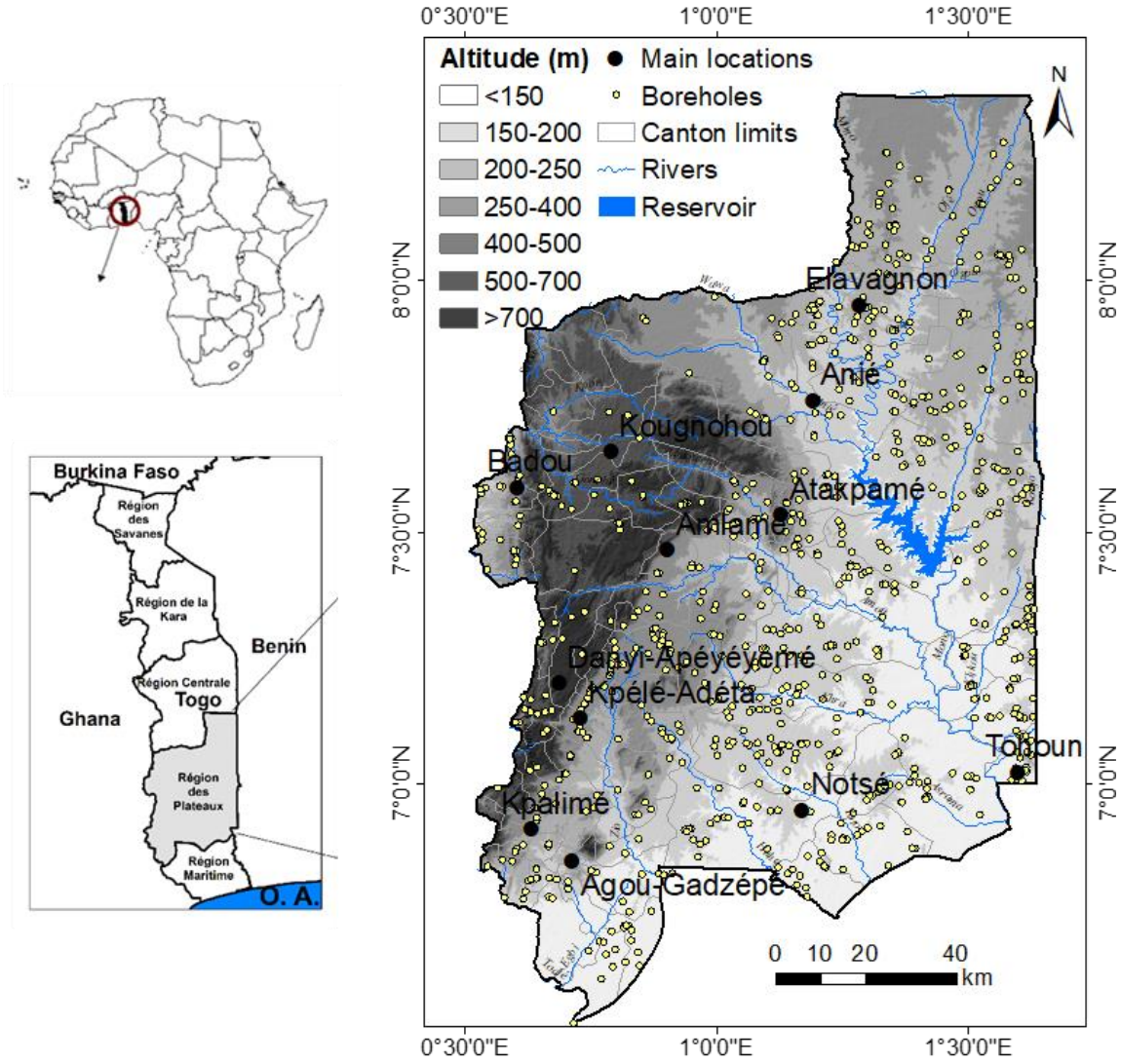

Figure 1. *Map showing the study area localization, relief, and boreholes.*

3. Material and Methods

3.1. Data Used

A hydrochemical database was constituted from over 900 boreholes water sampled and analyzed between 2007 and 2016 for physicochemical variables (pH, EC, TDS, F^-, Ca^{2+}, Mg^{2+}, Na^+, K^+, HCO_3^-, Cl, NO_3^- and, SO_4^{2-}), using standards methods. The coordinates of these points were obtained from the Plateaux Region Board of Water Resources and during field investigations. Each water point is associated with the canton in which it is circumscribed (Figure 1). Only cantons with at least three (3) water points are considered. The median concentrations of the major constituents are then calculated for each canton. The general state of land use and land cover (Figure 2c) is extracted from the African land use database from Globcover images from the European Space Agency (ESA) [24]. These data and the geological [23], pedological [25], and rainfall [26] maps (Figure 2) are integrated into a GIS to extract each point and canton's physiographic or geo-environmental features.

3.2. Comparison Test

Using the STATISTICA software, the nonparametric Kruskal-Wallis test with a 95% confidence level is applied to study the relationship between groundwater quality variables and the features of physiographic groups presented in Table 1 and Figure 2.

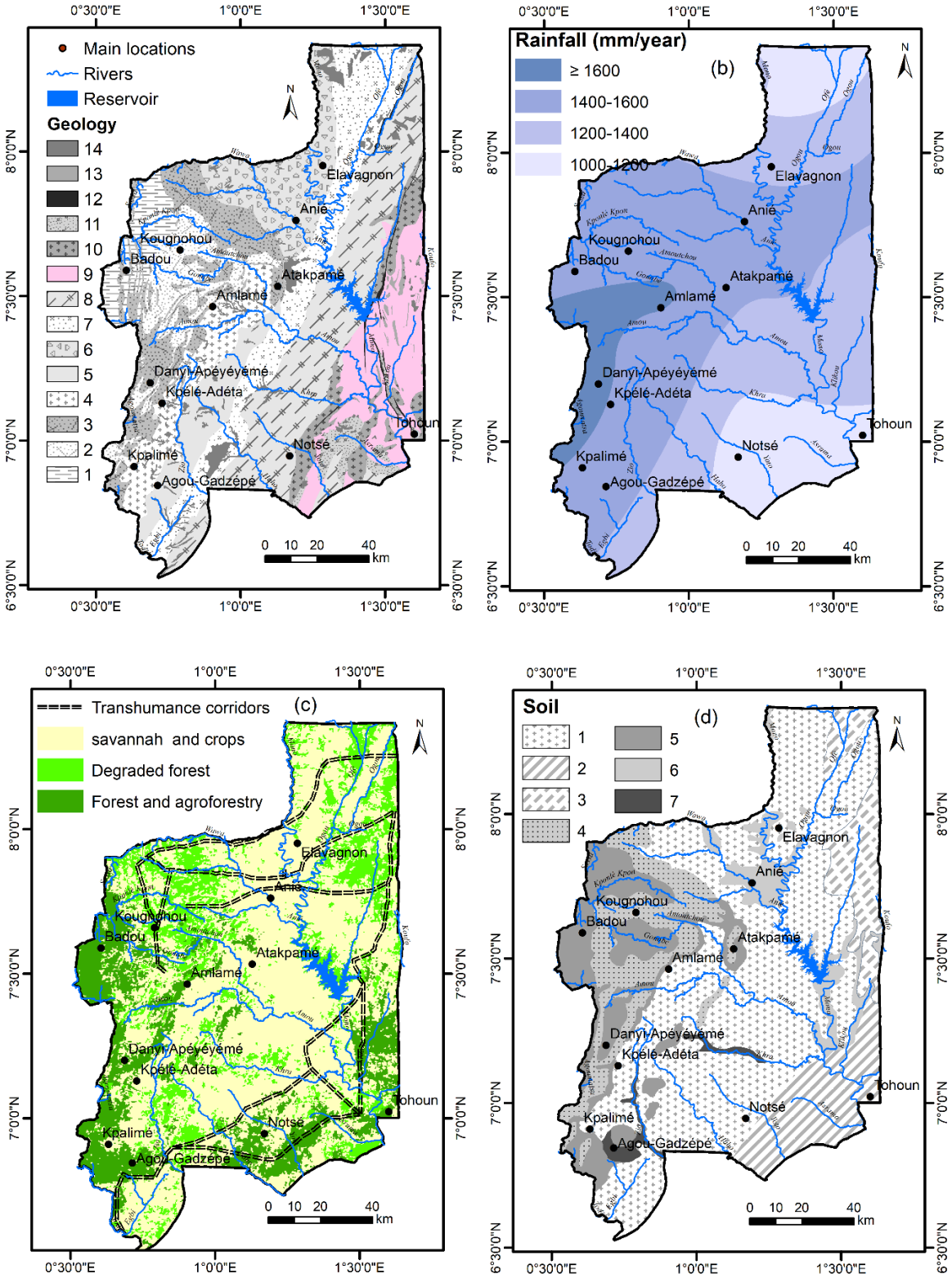

Figure 2. *Maps of the study area showing (a) Geological setting (Adapted from Sylvain et al., 1986). External Zone (1: Schists, 2: Quartzomicaschists, 3: Quartzites, 4: Pluto of the Amlamé-Palimé axis); Suture zone made up of basic and ultrabasic massifs (5: Atakpamé-Agou complex, 6: Mononé-Akaba complex) Internal zone (7: Granitic gneiss, 8: Migmatites, 9: Dioritic gneiss, 10: Orthogneiss and Granitoids, 11: Paragneiss and meta-arenites, 12: Mylonites, 13: Crystalline dolomites) and surface formations (14: Alluvium and laterites) (b) Isohyets of Mean Annual Rainfall, (c) Land use and land cover, and (d) soil types (1: Ferruginous with concretions and cuirasses, 2: Juxtaposition of ferruginous soils with concretions and cuirasses and ferruginous soils with deep pseudogley, 3: Juxtaposition of ferruginous and ferralitic soils with concretions and cuirasses, 4: Erosion soils Lithosols, 5: Modal ferralitic, 6: Temporarily moist vertisols, 7: Hydromorphic soils).*

Table 1. Features in the considered physiographic groups.

physiographic groups	Features	Assigned code
Geological features	USA schist	1
	USA Quartzites and micaschist	2
	Granitoids of the Palim é-Amlam é Pluton	3
	Basic and ultrabasic massifs of the Atakpam é-Agou complex	4
	Basic and ultrabasic massifs of the Mono Ani é-Akaba complex	5
	Central granitic gneiss	6
	Migmatites	7
	Oriental dioritic gneiss	8
	Oriental orthogneiss and granitoids	9
	Paragneiss and meta-arenites	10
Hydroclimatic domains / Rainfall amount (mm)	1800-1600 in western highland	1
	1600-1400, from the Atacora mountains to the basics and ultrabasic complex	2
	1200-1400 central plain	3
	1000-1200 Savana areas in the south-eastern and north-eastern edges	4
Soils	Ferruginous with concretions and cuirasses	1
	Juxtaposition of ferruginous soils with concretions and cuirasses and ferruginous soils with deep pseudogley	2
	Juxtaposition of ferruginous and ferralitic soils with concretions and cuirasses	3
	Erosion soils Lithosols	4
	Modal ferralitic	5
	Temporarily moist vertisols	6
	Hydromorphic soils	7
Land use land cover (LULC)	Forest in the west mountainous areas	1
	Clear forest, agroforestry, and crop mosaics in the south-eastern	2
	degraded forest and crop mosaics	3
	Crops, shrub-grass, and woodland savannah	4

3.3. Spatial Statistics

The spatial autocorrelations statistics were examined to determine the similarities and patterns in the spatial distribution of the median chemical composition of groundwater quality assigned as attributes to the cantons of the study area. A holistic analysis of the patterns displayed by cantons allows for describing the relationship with physiographic features. The selected techniques include the global Moran'I index for autocorrelation analysis, the local Getis-Ord Gi* statistics for hotspot analysis, and the Anselin Local Moran's I index for cluster and outlier analysis [27]. The following references [16, 17, 27, 28] provide the details of these spatial statistics.

Global Moran's index

Moran's Index is the more popular test statistic for spatial autocorrelation. Global Moran's I examines whether a spatial correlation exists over an entire region. It assesses the overall pattern and structure of spatial relationships in the dataset and is calculated based on Equation (1).

$$I=\frac{n}{\sum_i^n\sum_j^n w_{ij}}\frac{\sum_i^n\sum_j^n w_{ij}\,(x_i-\bar{x})(x_j-\bar{x})}{\sum_i^n(x_i-\bar{x})^2} \quad (1)$$

Where n is the number of cantons in the whole region, x_i and x_j are the attributes values of features i and j, $\bar{x}$ the mean of x, and w_{ij} an element of spatial weights matrix w, is the

spatial weight between features i and j.

The value of Moran's I varies between 1 and -1. spatial random distribution is indicated by p-value > 0.05 and an index value to nill. When p-value < 0.05, positive values of Moran's I indicate a positive spatial correlation that is a clustering tendency, and the closer to 1, the higher the spatial agglomeration; negative values indicate a negative spatial correlation that is a dispersion tendency, and the closer to -1, the greater the spatial difference.

Getis-Ord Gi statistics*

Local autocorrelation examines similar or dissimilar values within a specific neighborhood or local area. Its understanding is crucial in spatial analysis as it helps identify patterns hidden in aggregated data. Local Getis-Ord G_i^* statistics, also named hot spot analysis, identify if low or high values of an attribute are spatially clustered and create cold spots or hot spots, respectively. The Getis-Ord G_i^* index is obtained using Equation (2).

$$G_i^* = \frac{\sum_j w_{ij}(d)x_j}{\sum_{j=1}^{n} x_j} \quad (2)$$

Where n is the number of cantons in the whole region, x_j is the attribute value of feature j, w_{ij} an element of spatial weights matrix w, is the spatial weight between features i and j, and *d* is the estimated range of observed spatial autocorrelation.

For each polygon, a z-score value is calculated along with a p-value to assess the statistical significance of the results. The results are rendered as a map of the% confidence level of 95%. A high positive z-score and a p-value < 0.05 indicate spatial clustering of high values representing a hot spot, whereas having a low negative z-score with a small p-value reveals spatial clustering of low values referring to the presence of cold spots. Both situations reflect a positive spatial autocorrelation. When p-values > 0.05 or Z-score values are near zero, the results are not statistically significant, meaning there is no indication of clustering, as the process might be random.

Anselin Local Moran's I index

Anselin Local Moran's I statistic refers to cluster and outlier analysis of local autocorrelation. The cluster and outlier analysis is similar to that of hot spot analysis. Both find local clusters of high and low values, but a cluster and outlier analysis also identifies local outliers or features that differ significantly from their neighbors [17].

$$I_i = \frac{n(x_i - \bar{x})\sum_j^n w_{ij}\ (x_j - \bar{x})}{\sum_i^n (x_i - \bar{x})^2} \quad (3)$$

The notations are the same as for Equation (1), but the corresponding values are from the local neighboring region. With the local Moran's I statistic analysis, five categories of local spatial autocorrelation can be distinguished. Two of these are spatial clusters, including high values surrounded by high values (High-High), and low values surrounded by low values (Low-Low) types. Two are spatial outliers, including high values surrounded by low values (High-low) and low values surrounded by high values (Low-high). The last type is spatial randomness, without significant spatial patterns at the corresponding weight matrix.

The spatial statistics tools of ArcGIS 10.7 software served as the platform for implementing the spatial autocorrelation analysis using canton polygon features and applying contiguity edge conceptualization, euclidean distance method, and row standardization since data refer to polygons. The result's reliability is supported by the number of canton polygons (total of 78), which is higher than the minimum of 30 spatial objects required for such analysis. [27].

4. Results and Discussion

4.1. Variation of Groundwater Quality Across Physiographic Groups

The descriptive statistics of hydrochemical parameters are presented in Table 2. Based on WHO guideline values [29] on the suitability of water for drinking purposes, the physicochemical quality of water is essentially limited by pH, NO_3^-, Mg^{2+}, F^-, K^+, TDS, Ca^{2+}, Na^+, Cl^- and SO_4^{2-} in 21, 22, 11, 9.5, 9, 8, 7, 4, 2, and 1% of groundwater samples (Table 2). Most of the variables presented high coefficients of variation reflecting the variation of groundwater quality over the study area, probably in a relationship with the combined effect of various geo-environmental features. This is supported by the Kruskal-Wallis test, revealing statistical differences ($p < 0.05$) among physiographic groups for each groundwater quality parameter (Table 2).

Table 2. *Results of the chemical composition of groundwater and nonparametric Kruskal-Wallis test.*

	Descriptive statistics							p-values from Kruskal-Wallis test			
	mean	Min	Max	SD	CV (%)	WHO standards	% out of permissible limits	Geology	Soil	Rainfall	LULC
pH	6.8	3.4	8.3	0.6	8.8	6.5-8.5	21	<0.01	<0.01	<0.01	<0.01
EC	693	14	5010	468	67.5		-	<0.01	<0.01	<0.01	<0.01

	Descriptive statistics							p-values from Kruskal-Wallis test			
	mean	**Min**	**Max**	**SD**	**CV (%)**	**WHO standards**	**% out of permissible limits**	**Geology**	**Soil**	**Rainfall**	**LULC**
TDS	514	20	3798	357	69.5	50-1000	8	<0.01	<0.01	<0.01	<0.01
Ca^{2+}	50.9	0.8	436	37.3	73.3	100	7	<0.01	<0.01	<0.01	<0.01
Mg^{2+}	26.5	0.5	161.1	19.5	73.6	50	11	<0.01	<0.01	<0.01	<0.01
Na^{+}	56.8	0.5	621	50.6	89.1	150	4	<0.01	<0.01	<0.01	<0.01
K^{+}	6.3	<DL	32.5	4	63.5	12	9	<0.01	<0.01	<0.01	<0.01
HCO_3^-	285.1	3.6	939.4	154.8	54.3			<0.01	<0.01	<0.01	<0.01
Cl^-	51.6	<DL	1253.2	84.2	163.2	250	2	<0.01	<0.01	<0.01	<0.01
SO_4^{2-}	30.7	<DL	980.5	82.3	268.1	400	1	<0.01	<0.01	<0.01	<0.01
NO_3^-	39.4	<DL	626.9	80.3	203.8	50	22	<0.01	<0.01	<0.01	<0.01
F-	0.72	<DL	2.4	0.48	67.2	1.5	9.5	<0.01	<0.01	<0.01	<0.01

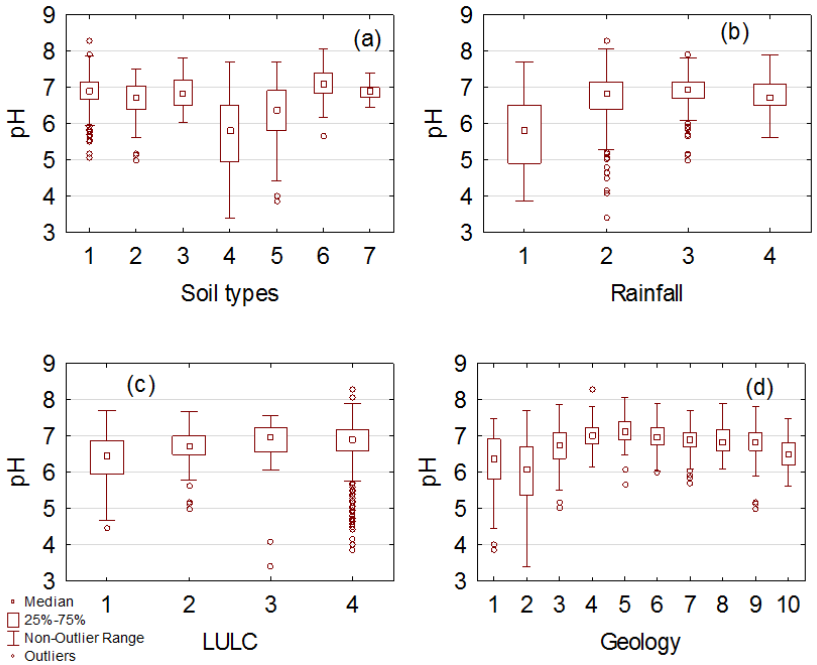

Figure 3. *pH relationship with physiographic features. The notations are described in Table 1.*

The pH of the groundwater samples ranged from 3.4 to 8.3, with a mean value of 6.8, suggesting acidic to slightly alkaline groundwater in the region. Other studies revealed the dominance of acidic groundwater in basement aquifers over West Africa, such as in Eastern Senegal [30] and southwest Nigeria [31]. The pH relationship with physiographic features is presented in Figure 3.

Groundwater is more acidic in the western part of the study area, particularly in the erosion soils Lithosols (Figure 3a) and quartzites and micaschist (Figure 3d) domain with a median value of around 6. These areas receive high rainfall amounts (Figure 3b). The relationship of groundwater pH with LULC features (Figure 3c) shows an association of acidic groundwater with forest and agroforestry zones. In contrast, the median pH values are circumneutral in degraded forests, shrub-grass savannahs, and crop mosaics. Acidic groundwater in forest and vegetation-dominated areas is also associated with high rainfall areas. The main proton source is the CO_2 release in root and soil zones that are in equilibrium with the shallow groundwater table [32], maintaining the release of carbonic acid in groundwater through CO_2 dissolution according to Equation (4).

$$CO_{2(g)} + H_2O \rightleftarrows H_2CO_{3(groundwater)} \quad (4)$$

Due to organic matter decomposition and other acidifying processes such as nitrification, acidic pH values are also present in shrub-grass savannah and crop mosaics. Still, most of the points are located in the study area's western part, suggesting the additional impact of surrounding forest and vegetation areas. The highest pH values indicating neutral to slightly basic groundwater, with a median of around 7.0, are found geologically in the basic and ultrabasic massif complexes. The alkaline pH of groundwater is usually found in ultrabasic massifs due to the serpentinization of ultrabasic rock, which involves the release of hydroxide ions into groundwater conditions at ambient temperature in open-system conditions close to the atmosphere [33, 34].

The electrical conductivity varied from 14 to 5010 µS/cm with a mean value of 693 µS/cm, suggesting fresh groundwater dominance. The relationship with physiographic features (Figure 4) reveals that areas with the predominance of low conductivity (< 1000 µS/cm) values are associated with erosion soils lithosols, modal ferralitic and the juxtaposition of ferruginous and ferralitic soils with concretions, and cuirasses soil types (Figure 4a). In general, mountainous forest zones with higher rainfall recorded the predominance of lower conductivity values in groundwater (Figure 3b), probably due to the high rate of groundwater recharge and fast fluxes or circulation driven by topographic gradients [35, 36]. This restricts the extent of water-rock interactions and solutes acquisition by groundwater. Based on the geology, groundwater presents lower mineralization in the western Atacora Structural Units. It is higher in the basic and ultrabasic massifs of the Atakpamé-Agou complex, the migmatites, and the orthogneiss formations. TDS and all ions except nitrate and fluoride relationships with the physiographic features (not shown) follow that of the electrical conductivity. All the parameter's median values increase with the decrease in rainfall, suggesting a contrast between dilution and evaporation effects on groundwater quality [37]. Higher Na^+ median concentrations are observed in granitic gneiss, migmatites, orthogneiss, granitoids, and paragneiss formations, probably due to the dominance of minerals such as plagioclase, amphibole, pyroxene with Na-rich end members [38]. The occasional high mineralization (> 2000 µS/cm) of groundwater is predominant in the migmatite formations (Figure 4d). Previous results in the region indicated that, in the central granitic gneiss, migmatites, and orthogneiss formations, the sandy weathering, flat slope, and savannah vegetation type favor water enrichment with solutes and a rapid transfer of ions to groundwater than in other parts of the study area where the weathering profile is deeper and clayey [39].

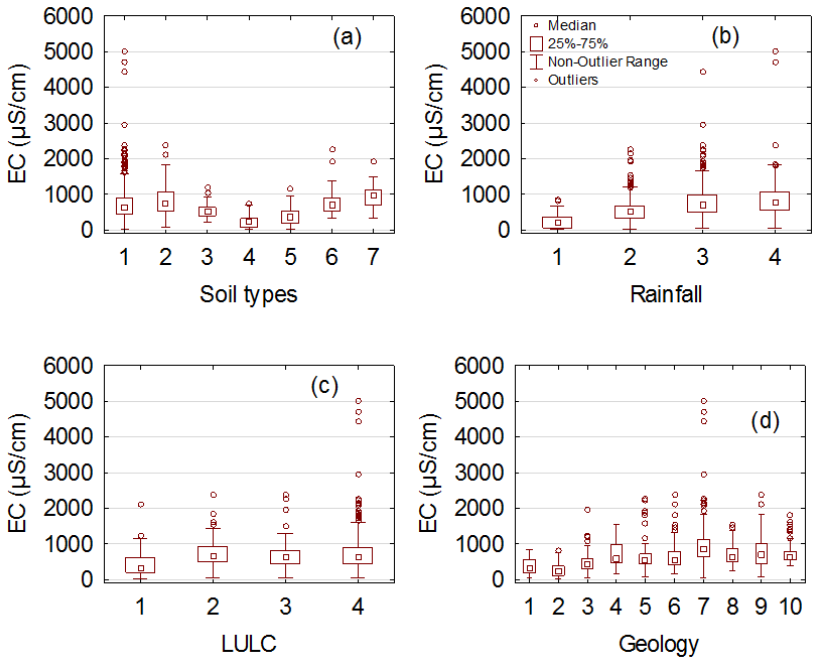

Figure 4. *EC relationship with physiographic features. The notations are described in Table 1.*

Nitrate is one of the main groundwater pollutants with deleterious human health risks. High nitrate concentrations in groundwater can cause methemoglobinemia or induce several types of cancer [29, 40]. Nitrate concentration varied from the detection limit to 626.9 mg/L, with a mean value of 39.4. The relationship with physiographic features (Figure 5) differs from the other ions, probably due to different sources and biogeochemical processes.

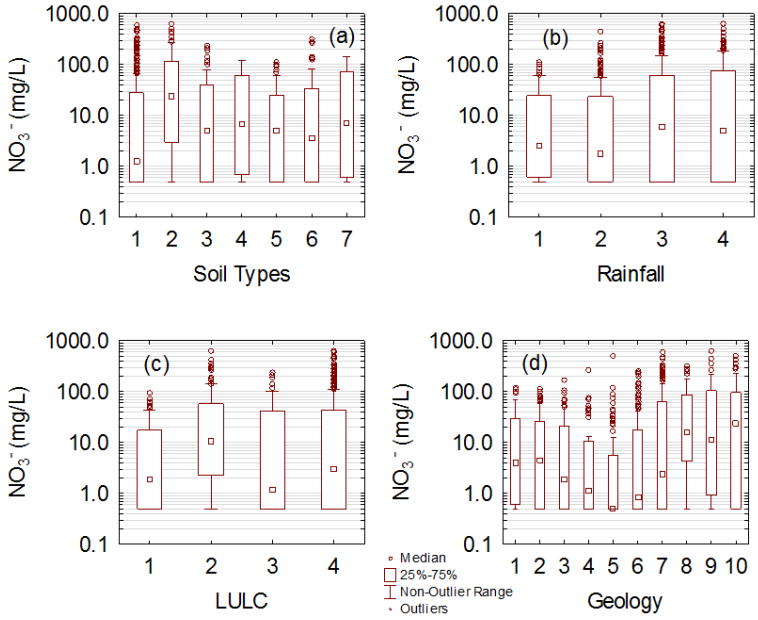

Figure 5. *NO_3^- relationship with physiographic features. The notations are described in Table 1.*

Groundwater is less contaminated in areas with higher rainfall (Figure 5b). Based on soil types, the median concentration is lower than 2 mg/L in the ferruginous with concretions and curasse domain, and the higher median value of around 25 mg/L is in areas covered by a juxtaposition of ferruginous soils with concretions and cuirasses and ferruginous soils with deep pseudogley soil types (Figure 5a). These later soil types result from the rise of the water table. The agroforestry and crop mosaics are associated with higher nitrate contamination among LULC features (Figure 5c). Therefore, groundwater might become more vulnerable to anthropogenic contamination from the surface in these areas where manure and synthetic fertilizers are widely used [21]. Differences in nitrate concentration can mirror land use changes, and the main anthropogenic drivers of LULC changes include deforestation, expansion of agriculture, conversion of land to pasture, agriculture, and urbanization. Around agricultural livestock-keeping fields of Babati town, in Tanzania, farming activities and animal husbandry were depicted as a lead cause of nitrate enrichment in groundwater and surface water [41]. Nitrate can also originate from atmospheric deposition, but in areas similar to the study area, their contribution is usually at a lower rate compared to manure, sewage, and fertilizers [19, 42].

The geological formation exerts a substantial relationship with nitrate contamination. Nitrate concentration is lower than 10 mg/L in the basic and ultrabasic complex, probably due to local physiographic constraints on anthropogenic impact. These concentrations reflect background concentration with limited human activities influence. Similar concentrations were observed in the basic and ultrabasic massifs domain in the northern part of the country [43]. The western Atacora Structural Units, Palimé-Amlamé Pluton, and central gneiss concentrations are higher but predominantly lower than 50 mg/L. From the migmatites to oriental dioritic gneiss domains, the non-outlier's maximal concentration is around 200 mg/L (Figure 4d). Generally, groundwater under no or minor human influence recorded Nitrate-nitrogen lower than 3 mg/L equivalent to nitrate concentrations of 13.7 mg/L [44]. The region's eastern part appears more vulnerable to anthropogenic contamination, probably due to higher human activity pressure, water table rise, and sandy weathering profile [18]. The eastern plain has a long history of cotton cultivation, with increasing land area and use of fertilizers [21, 45], as well as the arrival of cattle from Sahelian countries [46]. The main transhumant corridor presented in Figure 2c describes the uncontrolled disposal of animal wastes in addition to those of local pastoral activities. It is known that the crops directly use less than 50% of the mineral or organic fertilizer nitrogen [47]. Thus, a large proportion of nitrogen gets mineralized in soil and reaches groundwater via leaching, reflecting legacies of long-term contamination from manures and synthetic fertilizers [47-49].

Another critical parameter of groundwater quality is Fluoride, a geogenic pollutant reported in groundwater in different countries, particularly in Africa, Asia, and Europe [50]. Higher fluoride provinces in Africa include countries sharing the East African Rift Valley [51, 52] and West African countries like Ghana, Nigeria, Côte d'Ivoire, Niger, Mauritanie, and Senegal [51, 53, 54]. Although fluoride is an essential trace element required for humans, fluoride optimal doses fall within a narrow range of 0.7 to 1.2 mg/L, benefiting teeth and bones' formation, maintenance, and favorable health [51]. It has severe human health implications, such as dental caries if drinking water levels are below 0.5 mg/L or dental and skeletal fluorosis if drinking water levels exceed 1.5 mg/L [29, 51, 53, 55]. In this study, concentrations varied from the detection limit to 2.4 mg/l with a mean value of 0.72 mg/L. About 9.5%

of samples exceeded 1.5 mg/L and 38.4% below 0.5 mg/L. These results indicate potential fluoride-related health risks in the study area. In general, in the case of raw groundwater consumption without artificial fluoridation of water supplies, lower fluoride in drinking water is compensated by intake from food and the use of fluorinated toothpaste [50]. The relationship of fluoride with physiographic features is presented in Figure 6.

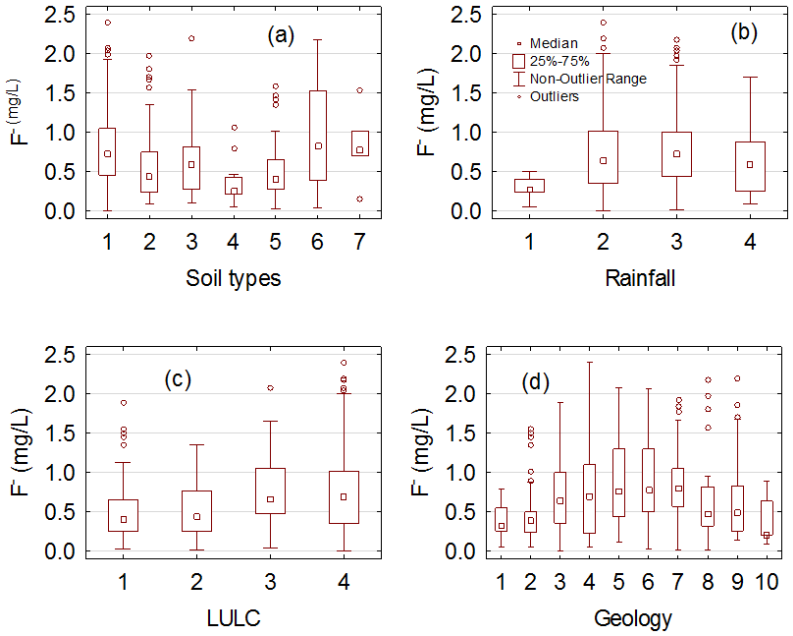

Figure 6. *Fluoride relationship with physiographic features. The notations are described in Table 1.*

The median concentrations above 0.5 mg/L are mainly associated with ferruginous and ferralitic soils with concretions and cuirasses, temporarily moist vertisols, and hydromorphic soil types (Figure 6a). In the highland and higher rainfall domain, corresponding to the Atacora Structural Units, concentrations were lowest below 0.5 mg/L. Concentrations were also low in the paragneiss and meta-arenites domain (Figure 6d). The primary geogenic sources of fluoride in groundwater are F-rich minerals such as fluorite, fluorapatite, villiaumite, sellaite cryolite, topaz, and bastnaesite [52]. In the basement aquifer, fluoride sources are related to the weathering of F-bearing minerals such as hornblende, biotite, amphibole, and muscovite, which are abundant in the study area rocks [23, 38, 56].

The median concentrations above 0.5 mg/L are associated with lower rainfall regions (Figure 6b) and savannah, shrub, and crop mosaic landscapes (Figure 6c). A decrease in groundwater fluoride with increasing altitude and rainfall was also observed in the northwest part of the Indo-Gangetic Basin [57]. Most of the fluoride pollution-prone zones are located in regions with arid and semi-arid climatic conditions through the evaporation process [50, 57]. Other factors affecting fluoride in groundwater are related to alkalinity and pH. Groundwater's alkaline nature favors hydroxide ions exchange with F-bearing minerals or compounds or fluoride adsorbed on the aquifer matrix. The examination of Figures 1 and 6 allows for detecting that physiographic features groups with fluoride median concentrations above 0.5 mg/L are associated with pH median values of around 7.0. This is consistent with the optimal pH (7 to 8) for releasing fluoride from muscovite and biotite [58].

4.2. Spatial Statistics

Table 3. *Results of the global spatial autocorrelation.*

	Global Moran's I	Z-scores	p-value
pH	0.43961	5.78538	0.00000
EC	0.59389	7.67116	0.00000
TDS	0.58269	7.56411	0.00000
Ca^{2+}	0.49667	6.59995	0.00000
Mg^{2+}	0.57201	7.23993	0.00000
Na^{+}	0.56935	7.44679	0.00000
K^{+}	0.56599	7.19623	0.00000
HCO_3^-	0.49519	6.28615	0.00000
Cl^-	0.51860	7.49322	0.00000
SO_4^{2-}	0.55588	7.64082	0.00000
NO_3^-	0.24531	3.55776	0.00037
F^-	0.21402	2.84997	0.00437

Table 3 presents the results of the spatial autocorrelation analysis of the median values of groundwater quality variables in the cantons in the study area. The z-scores are positive, and the p-values are statistically significant ($p < 0.05$), highlighting the spatial dependence or pattern in the data. Thus, the results unveil a significant spatial clustering of all the hydrochemical attributes. The dataset's spatial distribution of high and/or low values is more spatially clustered than expected if underlying spatial processes were random. Positive spatial autocorrelation dominated the whole study area. These results suggest a substantial variability in the chemical composition of groundwater due to a strong association with physiographic or geo-environmental features.

This confirmed that most measured variables do not follow a normal distribution, and concentrations are lower than the mean values for more than 50% of the collected samples. Thus, the high concentrations of ions, particularly nitrate, indicated contamination due to anthropogenic activities on a local scale. The central tendency values (e.g., mean) may not reflect the study area's groundwater chemistry. Thus, a spatial variability map of hydrochemical parameters in groundwater is necessary for drinking water quality management, particularly in a large-scale area. It helps delineate different water quality areas for each chemical constituent and prioritize the action zones for groundwater protection and contamination mitigation. It also provides the database for future comparison.

The results of the Anselin Local Morans I statistic examining the cluster and outlier analysis are resented in Figure 7. Figure 8 displays the median values in each canton and hotspot analysis results.

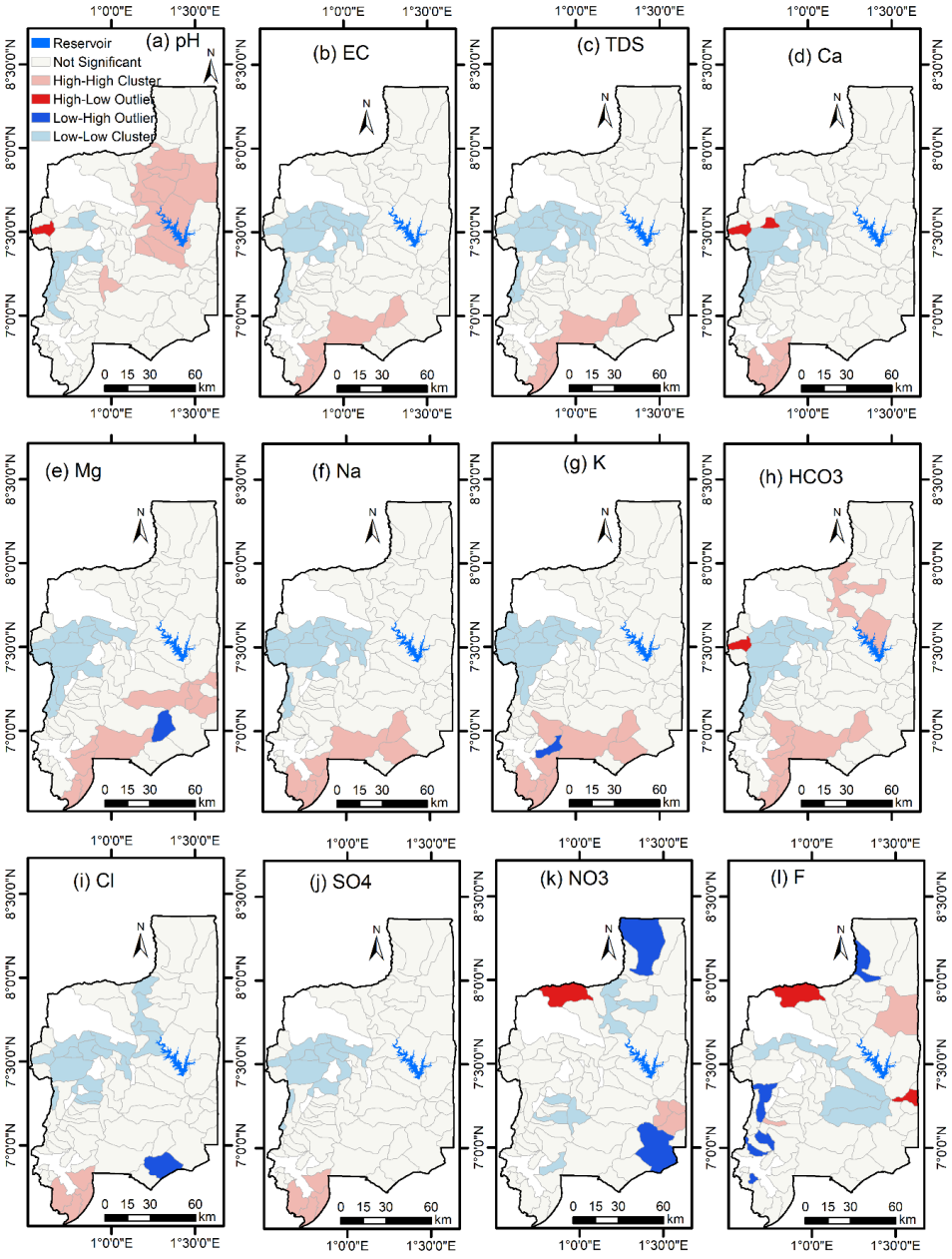

Figure 7. *Results of the cluster and outlier analysis.*

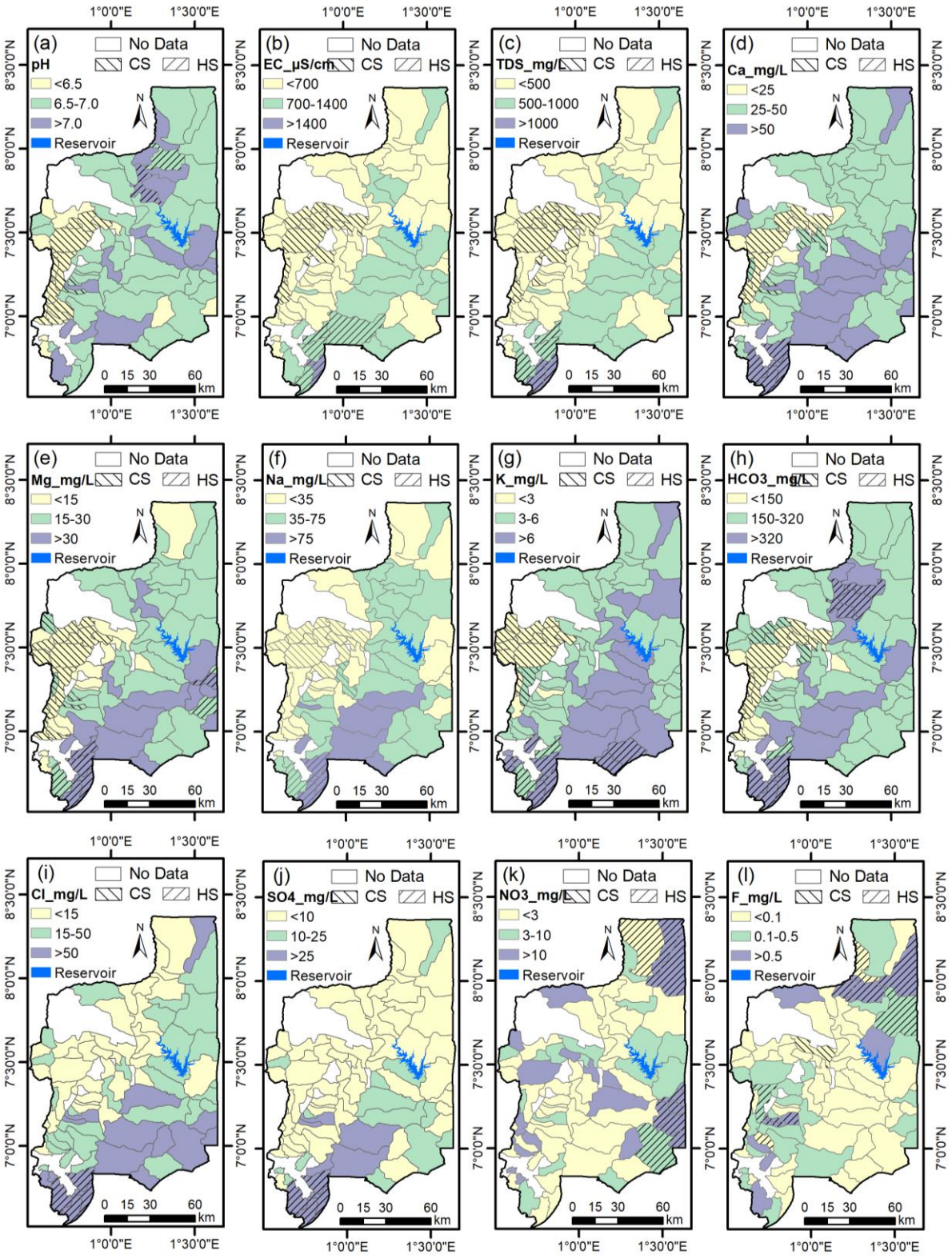

Figure 8. *Results of the hotspot analysis. CS = cold spot, and HS = Hot spot.*

The results show that groundwater in the western zone of the Region presents a significantly low mineralization ($p < 0.05$). In contrast, those in the south, the center, and sometimes in the east and north present a significantly more advanced mineralization. The Low-Low clusters and cold spots for most chemical attributes are located west of the study area characterized by higher rainfall, lithosols, forest, quartzites, and micaschist rocks. This part of the study area corresponds to the headwaters, which are expected to be essential sources of high-quality water, diluting nutrients, and other contami-

nants [59]. Similar low groundwater mineralization was found in the west Ghana border in these mountainous and forest lands, where recharge is as high as 20% of the precipitation [36].

Most cantons in the west of the Region have acidic groundwater with low pH values (< 6.5) (Figure 8a) and are aggregated at a confidence level of 95% as cold spots (Figures 7a and 8a). The pH hot spots are found in the north between Atakpamé and Elavagnon and in the south in the Agou (Figure 8a). They follow those in concentrations of bicarbonates (Figure 8h). The High-High cluster and hot spots for pH are located in the central part of the study area. The High-High clusters for EC, TDS, Na, and K are similar and developed southwestward (Figures 7b, c, f, and g). The hot spots regarding chloride and sulfate concentrations are in six cantons south of the Region. These are the cantons of Agotimé, Dzakpa, Amoussou Kopé, and Gadja in the prefecture of Agou and the cantons of Dalia and Atchavé in Haho along the transhumant corridor in the south (Figure 2c). Silicate minerals dominate the region. Thus, chloride and sulfate hot spots result from anthropogenic impacts such as sewage, domestic waste, agriculture, and livestock farming, which might exert control on the advanced evolution of groundwater chemistry [60]. This trend suggests that the high concentrations of these ions come from similar sources and factors in these cantons. Significant hotspots of chloride and sulfate concentrations appear to accompany those of sodium, potassium, and calcium. They are located in plain areas. Since groundwater flows from the mountainous headwaters or Piedmont zone toward lower land areas [18], these groundwater samples might also represent groundwater characteristics in discharge areas, in addition to anthropogenic influence. This situation denotes the hydrochemical evolution of groundwater associated with minerals weathering and dissolution reaching the aquifers along the flow path. Na and K enrichment with groundwater mineralization depends on the intensifying silicate minerals (for example, plagioclases, biotite, and amphibole) weathering, calcite and dolomite precipitation, and cation exchange (Ca^{2+} + 2NaX→ CaX2 +2Na^{+}) due to prolonged water-rock interactions along the flow path [39, 57]. Ca, Cl^{-}, and SO_4^{2-} present the High-High clusters in the same area with similar shapes (Figures 6 d, i, and j), probably due to salinity and calcium input from anthropogenic influences and subsequent carbonate precipitation processes. Magnesium and bicarbonate hot spots follow other ions but are represented with pH in the east and north (Figures 7a, e, and h). The pH and HCO_3^- variations are generally due to the same geochemical processes. Thus, these chemical parameters refer to the importance of the CO_2-driven hydrolysis of ferromagnesian silicates as natural sources of groundwater alkalinity [60]. Long-term deforestation, overgrazing, and agriculture practices are the key anthropogenic factors controlling soil and groundwater alkalinization [61].

Fluoride hot spots correspond to high pH and HCO_3^- areas in the northern part of the study area and to the Pali-m é-Amlam é Pluton in the south-west, which consists of silica-rich to intermediate granitoids and enclaves of mafic igneous rocks and gneisses (Figures 8a, h, l). The granitoids display various facies from medium to high-K calc-alkaline magnesian series and are characterized by abundant hornblende, Na-rich feldspar, muscovite, biotite, and apatite [56]. Weathered basement aquifers with such mineralogical composition host an abundance of geogenic sources of fluoride and sodium, which is considered conducive to groundwater fluoride enrichment [62]. Several studies have demonstrated that high fluoride concentrations in groundwater are associated with increasing sodium and alkalinity in groundwater and the interplay of Na^{+} release and Ca^{2+} removal [50, 51, 54, 57].

The hotspots for nitrate concentrations are located at the southeast and northeast ends of the Region. Other cantons relocated to the rest of the Region also tend towards high vulnerability (median NO_3^- concentrations higher than 10 mg/L) but do not constitute hot spots. The vulnerable zones are significantly associated with rainfall and the juxtaposition of meta-sedimentary formations with varieties of gneiss enclosing a procession of granitic intrusions. The granitic and meta-sedimentary formations are characterized by less clayey alteration, thus favoring the formation of more or less sandy soils and significant leaching of contaminants from surface origin [39]. Granite intrusions can also cause fractures to open more widely, making the transfer of solutes more effective. Significantly vulnerable cantons have a land use intensity generally above 50%. This implies a high use of agricultural inputs or overexploitation of soils, leading to the loss of fertility and capacity to store carbon and nutrients. Thus, a significant part of anthropogenic nitrogen inputs would be leached into the groundwater. Examining the relationships between groundwater nitrate concentrations in drinking water and landscape characteristics, [48] identified three categories of critical correlated variables that are related to contamination source (manure, sewage, and high agricultural nitrogen inputs), soil vulnerability conditions (low soil organic carbon and high hydraulic conductivity), and transport mechanisms (rapid and high aquifer recharge and groundwater mixing). However, it should be noted that factors such as the positioning of the hydraulic structures with settlements and pastures lands, the efficiency of the boreholes construction, and their maintenance could also significantly influence groundwater contamination [63]. The elaboration of nitrate directives and their implementation with targeted strategies according to local conditions are required to reduce nitrate concentrations and hotspots [49].

5. Conclusion

This study highlighted a significant variability in the chemical composition of groundwater depending on physiographic or geo-environmental features related to geology, soils, rainfall, and LULC in the Plateaux Region of Togo,

using the cantons' median concentrations of hydrochemical variables. It shows that water quality is limited by pH characterizing acidic water, TDS values indicating defects or excess water mineralization, excessive nitrate concentrations due to anthropogenic impact, and fluoride contamination from both geogenic and anthropogenic sources. The canton median values of physicochemical parameters are generally distributed in significantly hot spot zones in the lowland plain and significantly cold spot zones in the mountainous and forest parts. The region's southwestern to northern part represents geological and alkalinization-driven fluoride contamination hotspot zones. Nitrate contamination spread over the study area, but the East and the North are the main hot spots of contamination. The spatial statistics indicate significant global and local autocorrelations but are not stationary, thus showing the need to develop management strategies specific to each part of the study area. This study applied a simplistic approach that suits the current way of managing drinking water supplied from village boreholes. However, other socioeconomic and environmental factors must be considered to test the complexity of the basement aquifer vulnerability in the Plateaux Region of Togo.

Abbreviations

LULC	Land Use/Land Cover
WHO	World Health Organization

Acknowledgments

We thank the PIMASO Program, DAAD, and the SWINDON EXCEED Project for supporting the first author's research activities.

Conflicts of Interest

The authors declare no conflicts of interest.

References

[1] S. H. Ahn, D. H. Jeong, M. Kim, T. K. Lee, H. -K. Kim, Prediction of groundwater quality index to assess suitability for drinking purpose using averaged neural network and geospatial analysis, Ecotoxicology and Environmental Safety 265 (2023) 115485. https://doi.org/10.1016/j.ecoenv.2023.115485

[2] Y. Badetiya, M. Barale, Modeling groundwater level using geographically weighted regression, Arab J Geosci 17 (2024) 251. https://doi.org/10.1007/s12517-024-12051-x

[3] C. L. Chang, W. H. Kuan, P. S. Lui, C. Y. Hu, Relationship between landscape characteristics and surface water quality, Environ Monit Assess 147 (2008) 57-64. https://doi.org/10.1007/s10661-007-0097-1

[4] H.-F. Yeh, J.-C. Chang, C.-C. Huang, H.-Y. Chen, Spatial correlation of groundwater level with natural factors using geographically weighted regression model in the Choushui River Alluvial Fan, Taiwan, Front. Earth Sci. 10 (2022). https://doi.org/10.3389/feart.2022.977611

[5] E. A. Kudamnya, A. Edet, A. S. Ekwere, Analysing principal components of physiographic factors affecting groundwater occurrences within Keffi, North –Central Nigeria, The Egyptian Journal of Remote Sensing and Space Science 24 (2021) 665-674. https://doi.org/10.1016/j.ejrs.2021.08.005

[6] D. Machiwal, V. Cloutier, C. Güler, N. Kazakis, A review of GIS-integrated statistical techniques for groundwater quality evaluation and protection, Environ Earth Sci 77 (2018) 681. https://doi.org/10.1007/s12665-018-7872-x

[7] J. Gao, Z. Zhang, Y. Hu, J. Bian, W. Jiang, X. Wang, L. Sun, Q. Jiang, Geographical Distribution Patterns of Iodine in Drinking-Water and Its Associations with Geological Factors in Shandong Province, China, International Journal of Environmental Research and Public Health 11 (2014) 5431-5444. https://doi.org/10.3390/ijerph110505431

[8] J. Tu, Z.-G. Xia, Examining spatially varying relationships between land use and water quality using geographically weighted regression I: Model design and evaluation, Science of The Total Environment 407 (2008) 358-378. https://doi.org/10.1016/j.scitotenv.2008.09.031

[9] E.-H. Koh, E. Lee, K.-K. Lee, Application of geographically weighted regression models to predict spatial characteristics of nitrate contamination: Implications for an effective groundwater management strategy, Journal of Environmental Management 268 (2020) 110646. https://doi.org/10.1016/j.jenvman.2020.110646

[10] K. A. Alqadi, L. Kumar, H. M. Khormi, Mapping hotspots of underground water quality based on the variation of chemical concentration in Amman, Zarqa and Balqa regions, Jordan, Environ Earth Sci 71 (2014) 2309-2317. https://doi.org/10.1007/s12665-013-2632-4

[11] S. Caizhi, C. Xiangtao, C. Xuejiao, Evaluation and Hotspots Identification of Shallow Groundwater Contamination Risk in the Lower Reaches of the Liaohe River Plain, Journal of Resources and Ecology 7 (2016) 51-60. https://doi.org/10.5814/j.issn.1674-764X.2016.01.007

[12] Z. Islam, M. Ranganathan, M. Bagyaraj, S. K. Singh, S. K. Gautam, Multi-decadal groundwater variability analysis using geostatistical method for groundwater sustainability, Environ Dev Sustain 24 (2022) 3146-3164. https://doi.org/10.1007/s10668-021-01563-1

[13] K. Mahmood, R. Batool, Comparison of stochastic and traditional water quality indices for mapping groundwater quality zones, Environ Earth Sci 79 (2020) 405. https://doi.org/10.1007/s12665-020-09148-3

[14] S. Mohamadi, M. Honarmand, S. Ghazanfari, R. Hassanzadeh, Hotspot and accumulated hotspot analysis for assessment of groundwater quality and pollution indices using GIS in the arid region of Iran, Environ Sci Pollut Res 30 (2023) 69955-69976. https://doi.org/10.1007/s11356-023-27177-w

[15] B. Mtshawu, J. Bezuidenhout, K. Kilel, Spatial autocorrelation and hotspot analysis of natural radionuclides to study sediment transport, Journal of Environmental Radioactivity 264 (2023) 107207. https://doi.org/10.1016/j.jenvrad.2023.107207

[16] X.-N. Huo, H. Li, D.-F. Sun, L.-D. Zhou, B.-G. Li, Combining Geostatistics with Moran's I Analysis for Mapping Soil Heavy Metals in Beijing, China, International Journal of Environmental Research and Public Health 9 (2012) 995-1017. https://doi.org/10.3390/ijerph9030995

[17] L. Bennett, Spatial Statistics Illustrated, Esri Press, 2023. https://www.esri.com/en-us/esri-press/browse/spatial-statistics-illustrated (accessed September 27, 2024).

[18] K. V. Akpataku, Contributions of hydrogeochemistry and isotope hydrology to understanding aquifer functioning in basement zones in the Plateaux Region of Togo, PhD thesis, University of Lomé, Togo, 2018.

[19] J. Halder, K. V. Akpataku, L. M. Bawa, G. Djaneye-Boundjou, S. Faye, Multi-isotope approach to identify sources and fate of nitrate in the Plateaux Region of Togo, Geophysical Research Abstracts 21 (2019) 1.

[20] INSEED-Togo, Final results of the 5th General Census of Population and Housing (RGPH-5) of November 2022: Spatial distribution of the resident population by gender, National Institute for Statistics, Economic and Demographic Studies, Lomé, Togo, 2023.

[21] E. Kola, Recent trends of maize production in the Plateaux Region of Togo: trends, foundations, and constraints, Àhɔ̃h ɔ̃ (2012) 104-120.

[22] C. Castaing, A. Aregba, P. Assih-Edeou, P. Chevremont, K. S. Godonou, J. P. Sylvain, Gneissic units and crustal shear zone of South Togo, Journal of African Earth Sciences (and the Middle East) 7 (1988) 821-828. https://doi.org/10.1016/0899-5362(88)90025-5

[23] J. P. Sylvain, J. Collart, A. Aregba, S. Godonou, Explanatory note for the 1/500.0000 geological map of Togo General Directorate of Mines and Geology and National Mining Research Bureau, Collection N °6, 1986.

[24] O. Arino, J. Ramos, V. Kalogirou, P. Defourny, A. Fr édéric, Globcover 2009, Proc. ESA Living Planet Symp. (2010) 686-689.

[25] M. Lamouroux, Soil map of Togo at 1:1,000,000 (1969).

[26] T. C. Addra, A. K. Fahem, T. De Jong, T. Mank, ATLAS of regional development in Togo, Plateaux region, Editogo, Lomé, Togo, 1987.

[27] G. Grekousis, Spatial Analysis Methods and Practice: Describe - Explore - Explain through GIS, Cambridge University Press, 2020. https://doi.org/10.1017/9781108614528 (accessed September 23, 2024).

[28] A. Mitchell, A. Mitchell, L. S. Griffin, L. S. Griffin, The Esri Guide to GIS Analysis, Volume 2: Spatial Measurements and Statistics, second edition, Esri Press, 2020. https://www.esri.com/en-us/esri-press/browse/the-esri-guide-to-gis-analysis-volume-2-spatial-measurements-and-statistics-second-edition (accessed September 27, 2024).

[29] WHO, Guidelines for drinking-water quality: incorporating the first and second addenda, World Health Organization, Geneva, Switzerland, 2022. https://books.google.com/books?hl=fr&lr=&id=x3RyEAAAQBAJ&oi=fnd&pg=PR3&ots=73TphxTQd7&sig=lLVAg1yIE6nzASYe-6TapHjGc9A (accessed June 22, 2024).

[30] S. Diop, M. N. Tijani, Assessing the basement aquifers of Eastern Senegal, Hydrogeology Journal 16 (2008) 1349-1369. https://doi.org/10.1007/s10040-008-0353-7

[31] T. B. Adebayo, T. P. Abegunrin, G. O. Awe, K. S. Are, H. Guo, O. E. Onofua, G. A. Adegbola, J. O. Ojediran, Geospatial mapping and suitability classification of groundwater quality for agriculture and domestic uses in a Precambrian basement complex, Groundwater for Sustainable Development 12 (2021) 100497. https://doi.org/10.1016/j.gsd.2020.100497

[32] I. Clark, Groundwater geochemistry and isotopes, CRC press, Boca Raton, London, New York, 2015.

[33] S. Demer, Geological Genesis of Alkaline Magnesium-Type Groundwater within the Ophiolitic Rocks Areas in Southwestern Turkey, J. Earth Sci. 34 (2023) 1231-1248. https://doi.org/10.1007/s12583-022-1767-1

[34] Yu. A. Taran, D. P. Savelyev, G. A. Palyanova, B. G. Pokrovskii, Alkali Waters of the Ultrabasic Massif of Mount Soldatskaya, Kamchatka: Chemical and Isotopic Compositions, Mineralogy, and 14C Age of Travertines, Dokl. Earth Sc. 510 (2023) 262-268. https://doi.org/10.1134/S1028334X23600093

[35] L. E. Condon, R. M. Maxwell, Evaluating the relationship between topography and groundwater using outputs from a continental-scale integrated hydrology model, Water Resources Research 51 (2015) 6602-6621. https://doi.org/10.1002/2014WR016774

[36] A. Gibrilla, D. Adomako, G. Anornu, S. Ganyaglo, T. Stigter, J. R. Fianko, S. P. Rai, A. Ako, δ18O and δ2H characteristics of rainwater, groundwater and springs in a mountainous region of Ghana: implication with respect to groundwater recharge and circulation, Sustainable Water Resources Management (2017). https://doi.org/10.1007/s40899-017-0107-6

[37] S. K. Gurmessa, D. J. MacAllister, D. White, I. Ouedraogo, D. Lapworth, A. MacDonald, Assessing groundwater salinity across Africa, Science of The Total Environment 828 (2022) 154283. https://doi.org/10.1016/j.scitotenv.2022.154283

[38] G. Alayi, S. Kpanzou, Y. Agbossoumondé, E. Padaro, R.-P. Ménot, M. Tairou, Petrology, Age and Geodynamic Implication of the Panafrican Granitoids Associated with the Glito-Kpatala Shear Zone (South-East Togo), International Journal of Geosciences 14 (2023) 1193-1225.

[39] K. V. Akpataku, S. P. Rai, M. D. -T. Gnazou, L. Tampo, L. M. Bawa, G. Djaneye-Boundjou, S. Faye, Hydrochemical and isotopic characterization of groundwater in the southeastern part of the Plateaux Region, Togo, Hydrological Sciences Journal 64 (2019) 983-1000. https://doi.org/10.1080/02626667.2019.1615067

[40] R. Picetti, M. Deeney, S. Pastorino, M. R. Miller, A. Shah, D. A. Leon, A. D. Dangour, R. Green, Nitrate and nitrite contamination in drinking water and cancer risk: A systematic review with meta-analysis, Environmental Research 210 (2022) 112988. https://doi.org/10.1016/j.envres.2022.112988

[41] C. L. Mallya, M. J. Rwiza, Influence of land use change on nitrate sources and pollutant enrichment in surface and groundwater of a growing urban area in Tanzania, Environ Earth Sci 80 (2021) 111. https://doi.org/10.1007/s12665-021-09386-z

[42] P. Lartsey, S. Ganyaglo, D. Adomako, P. Sakyi, A. Gibrilla, F. Barbecot, K. Lefebvre, E. Nsikanabasi, Tracing Nitrate Contamination Sources and Apportionment in North-Western Volta River Basin of Ghana Using a Multi-Isotopic Approach, Water, Air, & Soil Pollution 235 (2024) 123456789. https://doi.org/10.1007/s11270-024-07418-5

[43] S. Zoulgami, M. D. T. Gnazou, T. Kodom, G. Djaneye-Boundjou, M. Bawa, Physico-chemical study of groundwater in the Northeast of Kara region (Togo), Int. J. Biol. Chem. Sci. 9 (2015) 711-1724.

[44] G. Anornu, A. Gibrilla, D. Adomako, Tracking nitrate sources in groundwater and associated health risk for rural communities in the White Volta River basin of Ghana using isotopic approach (δ 15 N, δ 18 O NO 3 and 3 H), Science of The Total Environment 603-604 (2017) 687-698. https://doi.org/10.1016/j.scitotenv.2017.01.219

[45] N. L. Gayibor, Le Togo sous domination coloniale (1884-1960), Les Presses de l'UB, Lomé, Togo, 1997.

[46] T. T. K. Tchamiè, Les conflits sociaux liés à la transhumance et leur règlement au Togo, Revue CAMES, Série B, Sciences Sociales et Humaines 5 (2003) 103-116.

[47] Bijay-Singh, E. Craswell, Fertilizers and nitrate pollution of surface and ground water: an increasingly pervasive global problem, SN Appl. Sci. 3 (2021) 518. https://doi.org/10.1007/s42452-021-04521-8

[48] Q. F. Hamlin, S. L. Martin, A. D. Kendall, D. W. Hyndman, Examining Relationships Between Groundwater Nitrate Concentrations in Drinking Water and Landscape Characteristics to Understand Health Risks, GeoHealth 6 (2022) e2021GH000524. https://doi.org/10.1029/2021GH000524

[49] J. Serra, C. Marques-dos-Santos, J. Marinheiro, S. Cruz, M. R. Cameira, W. De Vries, T. Dalgaard, N. J. Hutchings, M. Graversgaard, F. Giannini-Kurina, L. Lassaletta, A. Sanz-Cobeña, M. Quemada, E. Aguilera, S. Medinets, R. Einarsson, J. Garnier, Assessing nitrate groundwater hotspots in Europe reveals an inadequate designation of Nitrate Vulnerable Zones, Chemosphere 355 (2024) 141830. https://doi.org/10.1016/j.chemosphere.2024.141830

[50] E. Shaji, K. V. Sarath, M. Santosh, P. K. Krishnaprasad, B. K. Arya, M. S. Babu, Fluoride contamination in groundwater: A global review of the status, processes, challenges, and remedial measures, Geoscience Frontiers 15 (2024) 101734. https://doi.org/10.1016/j.gsf.2023.101734

[51] K. M. K. Kut, A. Sarswat, A. Srivastava, C. U. Pittman, D. Mohan, A review of fluoride in african groundwater and local remediation methods, Groundwater for Sustainable Development 2-3 (2016) 190-212. https://doi.org/10.1016/j.gsd.2016.09.001

[52] F. Ligate, J. Ijumulana, A. Ahmad, V. Kimambo, R. Irunde, J. O. Mtamba, F. Mtalo, P. Bhattacharya, Groundwater resources in the East African Rift Valley: Understanding the geogenic contamination and water quality challenges in Tanzania, Scientific African 13 (2021) e00831. https://doi.org/10.1016/j.sciaf.2021.e00831

[53] M. Diedhiou, S. Ndoye, A. Diagne, A. Gauthier, S. Whonlich, S. Faye, P. L. Coustumer, Spatial Distribution and Potential Health Risk Assessment of Fluoride and Nitrate Concentrations in Groundwater from Mbour-Fatick Area, Western Central Senegal, JWARP 16 (2024) 695-719. https://doi.org/10.4236/jwarp.2024.1611039

[54] S. Y. Ganyaglo, A. Gibrilla, E. M. Teye, E. D.-G. J. Owusu-Ansah, S. Tettey, P. Y. Diabene, S. Asimah, Groundwater fluoride contamination and probabilistic health risk assessment in fluoride endemic areas of the Upper East Region, Ghana, Chemosphere 233 (2019) 862-872. https://doi.org/10.1016/j.chemosphere.2019.05.276

[55] W. M. Edmunds, P. L. Smedley, Fluoride in Natural Waters, in: O. Selinus, B. Alloway, J. A. Centeno, R. B. Finkelman, R. Fuge, U. Lindh, P. L. Smedley (Eds.), Essentials of Medical Geology: Revised Edition, Springer Netherlands, Dordrecht, 2013: pp. 311-336. https://doi.org/10.1007/978-94-007-4375-5_13

[56] Y. Agbossoumondé, R.-P. Ménot, J. L. Paquette, S. Guillot, S. Yéssoufou, C. Perrache, Petrological and geochronological constraints on the origin of the Palimé-Amlamé granitoids (South Togo, West Africa): A segment of the West African Craton Paleoproterozoic margin reactivated during the Pan-African collision, Gondwana Research 12 (2007) 476-488. https://doi.org/10.1016/j.gr.2007.01.004

[57] S. P. Rai, K. V. Akpataku, J. Noble, A. Patel, S. Kumar Joshi, Hydrochemical evolution of groundwater in northwestern part of the Indo-Gangetic Basin, India: A geochemical and isotopic approach, Geoscience Frontiers 14 (2023) 101676. https://doi.org/10.1016/j.gsf.2023.101676

[58] A. Saxena, Fluoride Contamination in Groundwater and the Source Mineral Releasing Fluoride in Groundwater of Indo-Gangetic Alluvium, India, in: C. M. Hussain (Ed.), Handbook of Environmental Materials Management, Springer International Publishing, Cham, 2019: pp. 209-245. https://doi.org/10.1007/978-3-319-73645-7_128

[59] R. Kaule, B. S. Gilfedder, Groundwater Dominates Water Fluxes in a Headwater Catchment During Drought, Front. Water 3 (2021). https://doi.org/10.3389/frwa.2021.706932

[60] K. V. Akpataku, M. D. T. Gnazou, G. Djanéyé-Boundjou, L. M. Bawa, S. Faye, Role of Natural and Anthropogenic Influence on the Salinization of Groundwater from Basement Aquifers in the Middle Part of Mono River Basin, Togo, Journal of Environmental Protection 11 (2020) 1030-1051. https://doi.org/10.4236/jep.2020.1112065

[61] L. Wang, K. Seki, T. Miyazaki, Y. Ishihama, The causes of soil alkalinization in the Songnen Plain of Northeast China, Paddy Water Environ 7 (2009) 259-270. https://doi.org/10.1007/s10333-009-0166-x

[62] M. J. Addison, M. O. Rivett, P. Phiri, P. Mleta, E. Mblame, M. Banda, O. Phiri, W. Lakudzala, R. M. Kalin, Identifying Groundwater Fluoride Source in a Weathered Basement Aquifer in Central Malawi: Human Health and Policy Implications, Applied Sciences 10 (2020) 5006. https://doi.org/10.3390/app10145006

[63] T. Foster, Predictors of sustainability for community-managed handpumps in sub-Saharan Africa: evidence from Liberia, Sierra Leone, and Uganda, Environmental Science & Technology 47 (2013) 12037-12046.